Original Article

Synthesis, Antioxidant, and Anti-tyrosinase Activity of Some Aromatic Oximes: An Experimental and Theoretical Study

Rafik Bensegueni[1,2], Mounia Guergouri[2], Chawki Bensouici[3], Mustapha Bencharif[2]

[1]Université Mohamed Cherif Messaadia, Souk Ahras, Algeria, [2]Laboratoire de Chimie des Matériaux Constantine, Université Frères Mentouri Constantine 1, Constantine, Algeria, [3]Centre de Recherche en Biotechnologie, Constantine, Algeria

Abstract

In this study, five oximes were synthesized, characterized, and their antioxidant activity investigated experimentally and theoretically. Labeled OX1–OX5, our oximes were subjected to three antioxidant activity assays (1,1-diphenyl-2-picrylhydrazyl, cupric reducing antioxidant capacity test [CUPRAC], and ferric reducing antioxidant power test). The related results were very fulfilling presenting certain antioxidant properties for the majority of the studied compounds, especially with CUPRAC test where OX1 and OX2 presented a better result than the used standard antioxidants. Besides, the thermodynamic molecular descriptors (bond dissociation enthalpy, ionization potential, and proton affinity) of our molecules were calculated with the density functional theory to elucidate the experimental results. The resulting values were in a good agreement with the experimental results. The second part of this work consisted of an anti-tyrosinase activity evaluation of the five oximes where three of them displayed an inhibitory effect against this enzyme. To analyze this result, a molecular docking was conducted and the obtained values were in accordance with the experience. Absorption, distribution, metabolism, and excretion properties were also assessed via Molinspiration software and all our molecules satisfied the related conditions. Thus, the conducted theoretical and experimental studies were in excellent harmony, together supporting the antioxidant power of our compounds, which could permit their use in cosmetic, pharmaceutical, or food industry domains, after further clinical tests.

Keywords: *Antioxidant activity, anti-tyrosinase activity, density functional theory calculations, molecular docking, oximes*

Key messages:

- The majority of our oximes showed a good antioxidant activity.
- OX3, OX4, and OX1 revealed an anti-tyrosinase activity.
- The same result is obtained theoretically.

Introduction

The existence of free radicals in the human body is essential for the immune defense. However, the excess of these can be harmful to health. Hence, the pharmacological search for new and more efficient antioxidant agents remains essential. Oximes are compounds characterized by the general structure R'R"C = N-OH, which have been widely studied. Their antioxidant activity was investigated and shown in various studies[1-3] such as in the case of naringenin-oxime where the addition of the oxime group has increased the antioxidant activity of pure naringenin.[4] They are also used in other therapeutic applications as in the antidotal treatment of poisoning by organophosphorus nerve agents.[5] However, the mechanism of antioxidant action of oximes has not been investigated enough theoretically. In this work, a set of five oximes, labeled OX1–OX5, were synthesized [Figure 1], characterized with proton nuclear magnetic resonance (^{1}H NMR), and then subjected to three antioxidant activity tests: 1,1-diphenyl-2-picrylhydrazyl (DPPH) scavenging activity test, cupric reducing antioxidant capacity test (CUPRAC), and ferric reducing antioxidant power test (FRAP).

In the context of the density functional theory (DFT), three thermodynamic molecular descriptors were calculated for the tested molecules, to propose the most favorable mechanism for the free radicals scavenging activity. The three possible mechanisms that may coexist are hydrogen atom transfer (HAT), single electron transfer–proton transfer (SET-PT), and sequential proton loss electron transfer (SPLET).[6,7] These mechanisms are defined by the next equations:

How to cite this article: Bensegueni R, Guergouri M, Bensouici C, Bencharif M. Synthesis, antioxidant and anti-tyrosinase activity of some aromatic oximes: an experimental and theoretical study. J Rep Pharm Sci 2019;8:195-203.

***Address for correspondence**: Prof. Mustapha Bencharif, Laboratoire de Chimie des Matériaux Constantine, Université Frères Mentouri Constantine 1, Constantine, Algeria.*
E-mail: m_bencharif@umc.edu.dz

Access this article online

Website: www.jrpsjournal.com

DOI:10.4103/jrptps.JRPTPS_46_18

Quick Response Code:

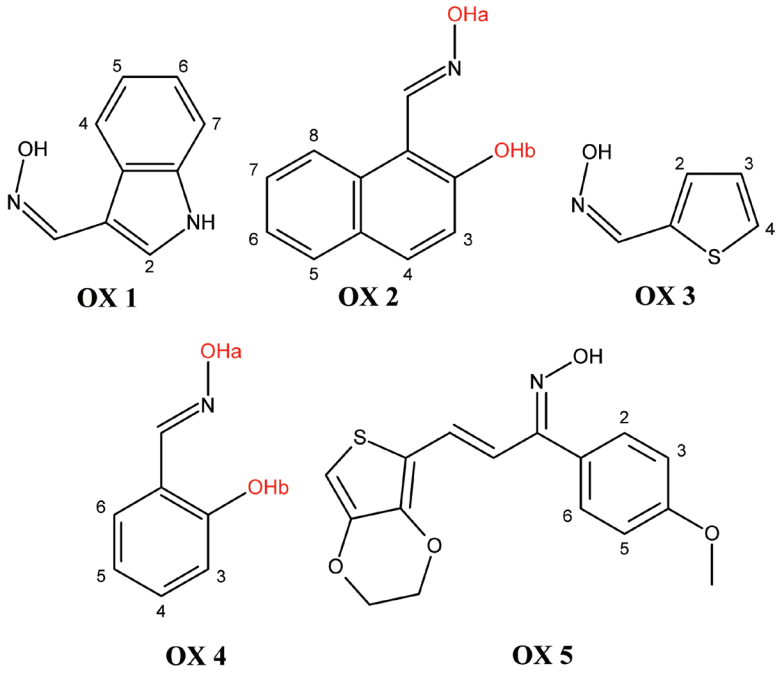

Figure 1: Chemical structures of the studied compounds

$$\text{HAT}: RX-H \rightarrow H^{\cdot} + RX^{\cdot}$$

$$\text{SET}-\text{PT}: \begin{cases} RX-H \rightarrow (RX-H)^{+\cdot} + e^{-} \\ (RX-H)^{+\cdot} \rightarrow RX^{\cdot} + H^{+} \end{cases}$$

$$\text{SPLET}: \begin{cases} RX-H \rightarrow RX^{-} + H^{+} \\ RX^{-} \rightarrow RX^{\cdot} + e^{-} \end{cases}$$

Each mechanism is characterized by one or more descriptors. Thus, HAT mechanism is related to the O–H bond dissociation enthalpy (BDE), when the first step of the SET–PT mechanism is controlled by the ionization potential (IP) and the second one is governed by the proton dissociation enthalpy (PDE) of the corresponding cation radical. For the SPLET mechanism, the proton affinity (PA) of the anion RX^{-} and the electron transfer enthalpy (ETE) are the enthalpies that manage the two steps of the mechanism, respectively. Therefore, BDE, IP, and PA are the main molecular descriptors, which determine the preferred antioxidant mechanism. The lower their values, the higher the scavenging activity.[8]

For CUPRAC and FRAP tests, the mechanism consists of an electron transfer from the studied molecule to the copper (II) complex and the iron (III) complex,[9] respectively. That is why the corresponding activities are related to the IP values of the tested compound, the higher is the IP value, the lower is the antioxidant activity.

Besides, the anti-tyrosinase activity of our oximes was evaluated experimentally. Afterward, the results thus obtained are analyzed and explained theoretically using a molecular docking calculation. Tyrosinase is a three copper enzyme (EC 1.14.18.1) found in different organisms from bacteria to animals.[10] It is implicated in the biosynthesis of melanin,[11] a defense pigment present in skin. Tyrosinase inhibitors, such as kojic acid conjugates, are commonly used in cosmetic industry against skin disease.[12] It should be noted that an anti-tyrosinase potency for some oximes has been shown.[13,14]

Materials and Methods

Materials

For synthesis: salicylaldehyde, 2-hydroxy-1-naphthaldehyde, 2-thiophenecarbaldehyde, 1H-indole-3-carbaldehyde, 3,4-ethylenedioxythiophene-2-carbaldehyde, 4-methoxyacetophenone, phenylhydrazine hydrochloride, pyridine, and absolute ethanol were obtained from Sigma-Aldrich (Sternheim, Germany). All products were used without further purification.

For antioxidant tests: 1,1-diphenyl-2-picrylhydrazyl (DPPH), butylated hydroxyanisole (BHA), butylated hydroxytoluene (BHT), neocuproine, trichloroacetic acid (TCA), potassium ferricyanide ($K_3Fe(CN)_6$), tyrosinase from mushroom (EC 1.14.18.1, ≥1000 unit/mg solid), l-DOPA (3,4-dihydroxy-l-phenylalanine), and kojic acid were obtained from Sigma-Aldrich, iron (III) chloride ($FeCl_3$), copper (II) chloride ($CuCl_2$), and ammonium acetate ($ACNH_4$) were obtained from Biochem Chemopharma, France. All other chemicals and solvents were of analytical grade.

All calculations were performed with Gaussian 9.0 software,[15] whereas GaussView 5.0.9 (Gaussian, Inc. Wallingford, CT 06492 USA)[16] was used for result visualization and analysis.

^{1}H NMR spectra were recorded on a Bruker Avance DPX 250 spectrometer with tetramethylsilane (TMS) as internal

reference. Measurements and calculations of the antioxidant activity were carried out on a 96-well microplate reader, PerkinElmer, France, Multimode Plate Reader EnSpire.

Synthesis

Preparation of oximes: Our compounds were synthesized by a condensation between an aldehyde (or a chalcone in the case of OX5) and an hydroxylamine. An equimolar mixture (0.04 mol) of hydroxylamine hydrochloride ($NH_2OH.HCl$), pyridine, and the carbonyl compound are dissolved in 20 mL of ethanol and refluxed for 3 h. The reaction is followed by thin layer chromatography. After evaporation of ethanol, the reaction mixture is taken up in ether and washed with a solution of HCl (10%) to remove the residual base. After washing with water until neutral pH, the organic phase is dried and evaporated in a vacuum and then recrystallized in ethanol to get the oxime [Scheme 1].[17]

Identification of 1H-indole-3-carbaldehyde oxime (OX1)

White fine needles, yield: 90%. Melting point (Mp): 195°C. ^{1}H NMR ($CDCl_3$, 250 MHz): 11.00 (s, 1H, N-H); 10.70 (s, 1H, NO-H); 7.85 (s, 1H, CH=N); 7.52 (s, 1H, H_2); 7.31(d, 1H, H_4, ^3J = 8.52 Hz); 7.03 (d, 1H, H_7, ^3J = 7.9 Hz); 6.55 (t, 2H, H_5, H_6, ^3J = 7.52–7.61 Hz). IR (cm^{-1}): 3380 (ν_{N-H}), 3047 (ν_{NO-H}), 3157–2745 (ν_{C-H}), 1635 ($\nu_{C=N}$), 1456 (ν_{N-O}), 1412 (δ_{C-C} in-the-plan), 1335 (ν_{C-N}), 1229 (ν_{N-O}), 1096 (ν_{C-N}), and 741 ($\gamma_{ortho\text{-}disubstituted\ aromatic}$ out of-the-plan).

Identification of 2-hydroxynaphthaldehyde oxime (OX2)

Light green powder, yield: 92%. Melting point (Mp): 157°C. ^{1}H NMR (DMSO-d6, 250 MHz): 11.6 (s, 1H, NO-H); 11.17 (s, 1H, O-H); 9.12 (s, 1H, CH=N); 8.50 (d, 1H, H_4, ^3J = 8.55 Hz); 7.83 (d, 2H, H_5, H_8, ^3J = 9.15 Hz); 7.52 (t, 1H, H_7, ^3J = 7.49 Hz);7.40 (t, 1H, H_6, ^3J = 7.35 Hz); 7.24 (d, 1H, H_3, ^3J = 8.9 Hz). IR (cm^{-1}): 3322 (ν_{O-H}), 3025 (ν_{NO-H}), 3010–2800 (ν_{C-H}), 1631 ($\nu_{C=N}$), 1589 ($\nu_{C=C}$), 1465 (ν_{N-O}), 1238 (ν_{C-O}), and 937 ($\delta_{C=C}$ out of-the-plan).

Identification of 2-thienylcarbaldehyde oxime (OX3)

White powder, yield: 82%. Melting point (Mp): 129°C. ^{1}H NMR ($CDCl_3$, 250 MHz): 8.95 (s, 1H, NO-H); 7.75 (s, 1H, CH=N); 7.60 (d, 1H, H_4, ^3J = 4.99 Hz); 7.43 (d, 1H, H_2, ^3J = 2.94 Hz); 7.13 (t, 1H, H_3, ^3J = 3.81–3.85 Hz). IR (cm^{-1}): 3157 ($\nu_{C-H\alpha}$), 3058 (ν_{NO-H}), 3050–2746 (ν_{C-H}), 1630 ($\nu_{C=N}$), 1428 ($\delta_{C-H\alpha}$ in-the-plan), 1412 (δ_{C-C} in-the-plan), 1228 (ν_{N-O}), 1047 (ν_{C-S}), and 935 ($\delta_{C=C}$ out of-the-plan).

Identification of 2-salicylaldehyde oxime (OX4)

Pale brown powder, yield: 69%. Melting point (Mp): 52–56°C. ^{1}H NMR (DMSO-d6, 250 MHz): 11.42 (s, 1H, NO-H); 10.20 (s, 1H, O-H); 8.40 (s, 1H, CH=N); 7.5(d, 1H, H_6, ^3J = 7.63 Hz); 7.25 (t, 1H, H_4, ^3J = 8.36 Hz); 6.90 (t, 1H, H_5, ^3J = 7.98 Hz); 6.86 (d, 1H, H_3, ^3J = 7.39 Hz). IR (cm^{-1}): 3379 (ν_{O-H}), 3076 (ν_{NO-H}), 3020–2800 (ν_{C-H}), 1620 ($\nu_{C=N}$), 1587 ($\nu_{C=C}$), 1496 (ν_{N-O}), 1257 (ν_{C-O}), 991 ($\delta_{C=C}$ out of-the-plan), and 740 ($\gamma_{ortho\text{-}disubstituted\ aromatic}$ out of-the-plan).

Identification of (E)-3-(3,4-ethylenedioxythienyl)-1-(4-methoxyphenyl)prop-2-en-1-one oxime (OX5)

Yellow powder, yield: 34%. Melting point (Mp): 126°C–127°C. ^{1}H NMR ($CDCl_3$, 250 MHz): 8.8 (s, 1H, NO-H); 7.82 (d, 1H, CH=C, J = 16.75 Hz); 7.77 (m, 2H, H_2, H_6); 7.37 (m, 2H, H_3, H_5); 7.08 (d, 1H, CH=C, J = 15.78 Hz); 7.01 (s, 1H, Hα); 4.40 (m, 4H, CH_2); 4.02 (s, 3H, CH_3). IR (cm^{-1}): 3167 ($\nu_{C-H\alpha}$), 3051 (ν_{NO-H}), 3025–2736 ($\nu_{C\text{-}Harom.}$), 2660–2646 ($\nu_{C\text{-}Halkanes}$), 1896 ($\gamma_{para\text{-}disubstituted\ aromatic}$ out of-the-plan), 1576 ($\nu_{C=N}$), 1468 (ν_{N-O}), 1187 (ν_{C-O}), 991 ($\delta_{C=C}$ out of-the-plan), and 705 (ν_{C-S}).

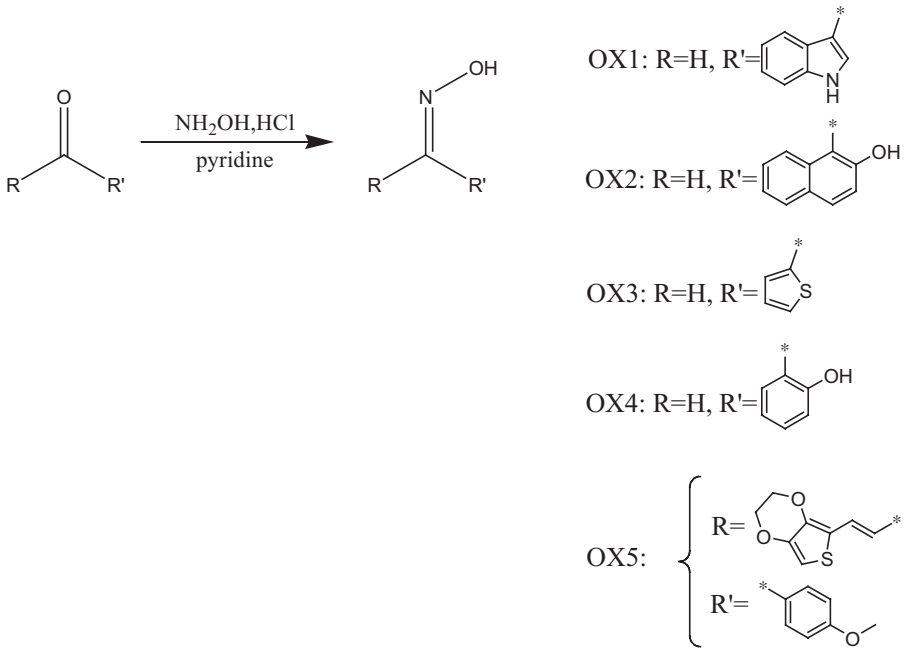

Scheme 1: Synthesis scheme of the studied oximes

Preparation of the precursor chalcone: In a round-bottomed flask, 3,4-ethylenedioxythiophene-2-carbaldehyde (5 mmol) and 4-methoxyacetophenone (5 mmol) were dissolved in 6 mL of ethanol. A total of 7 mL of 10% of NaOH were added, and the mixture was stirred at 60°C for 20 min. The mixture was cooled and poured in 50 g of ice water. The precipitate was filtered, washed with cold water, and dried [Scheme 2].

Identification of (E)-3-(3,4-ethylenedioxythenyl)-1-(4-methoxyphenyl)prop-2-en-1-one

Yellow powder, yield: 75%. Melting point (Mp): 130°C. ^{1}H NMR ($CDCl_3$, 250 MHz): 8.03 (d, 2H, H_2, H_6, ^3J = 8.8 Hz); 7.85 (d, 1H, CH=C, J = 15.31 Hz); 7.26 (d, 1H, CH=C, J = 15.33 Hz); 6.99 (d, 2H, H_3, H_5, ^3J = 8.83 Hz); 6.49 (s, 1H, Hα); 4.30 (m, 4H, CH_2); 3.91 (s, 3H, CH_3).

Antioxidant activity assessment

The antioxidant activity of the five oximes was tested using DPPH scavenging activity, CUPRAC, and FRAP power assays. BHA and BHT were used as positive standards.

1,1-Diphenyl-2-picrylhydrazyl scavenging activity method

The free radical-scavenging activity was determined by the DPPH assay.[18] Briefly, 40 µL of each sample solution prepared in ethanol at different concentrations was added to 160 µL of a DPPH ethanolic solution (0.1 mM). The mixture was left in darkness for 30 min. The absorbance was measured at 517 nm using microplate reader. BHT and BHA were used as antioxidant standards. The results were given as percentage of inhibition (or scavenging) of the initial DPPH at 100 µg/mL of the sample concentration. The percentage of inhibition was calculated by using the formula:

$$\text{Inhibition}(\%) = \frac{A_{Sample} - A_{Control}}{A_{Sample}} \times 100$$

Cupric reducing antioxidant capacity method

The cupric reducing antioxidant capacity was determined according to the method by Apak *et al.*[19] In each well, the reaction mixture containing 40 µL of our sample, 50 µL of copper (II) chloride solution, 50 µL of neocuproine alcoholic solution, and 60 µL of ammonium acetate aqueous buffer at pH 7. This mixture was left 30 min before measuring absorbance at 450 nm. The results were expressed as $A_{0.50}$ values (µg/mL), corresponding to the sample concentration indicating 0.5 absorbance.

Ferric reducing antioxidant power method

The method as described by Oyaizu[20] was used to estimate the reducing power activity of our compounds. A total of 10 µL of each sample solution at various concentrations were added to 40 µL of 0.2 M phosphate buffer (pH 6.6) and 50 µL of $K_3Fe(CN)_6$ (1%). Everything was incubated for 20 min at 50°C. A total of 50 µL of TCA (10%) and 10 µL of ferric chloride (0.1%) was added to the mixture and completed with 40 µL of distilled water. The ferric reducing antioxidant power was followed spectrophotometrically at 700 nm, and the $A_{0.50}$ values (µg/mL) were calculated.

All data on antioxidant activity test were the average of triplicate analyses. Data were recorded as the mean ± standard deviation. Significant differences between mean values were determined using Student's *t* test; *P* values <0.05 were regarded as significant.

Density functional theory calculations

Molecular modeling and geometry optimization

Molecular structures of the five molecules were optimized by DFT using B3LYP functional with the 6-311G(d,p) basis set. No geometrical constraints were applied. Frequency calculations were carried out at the same level of theory. Solvent effects were considered via the integral equation formalism variant of the polarizable continuum model (IEFPCM) salvation model.[21]

Descriptors calculation

Molecular descriptors are calculated using Equations (1)–(5) at 298.15 K and 1 atmosphere. For the gas phase, the enthalpy values of hydrogen atom ($H^{\cdot}$), proton (H^+) and electron (e^-) are equal to −1309.408 kJ/mol, 6.197 kJ/mol, and 3.145 kJ/mol, respectively.[22,23] In ethanol, the value of −1307.479 kJ/mol was used for the hydrogen atom enthalpy,[24] whereas those of proton and electron, $H(H^+_{sol})$ and $H(e^-_{sol})$, were obtained from the corresponding solvation enthalpies[25] and were equal to −1012.303 kJ/mol and −102.154 kJ/mol, respectively.

$$BDE = H(RX^{\cdot}) + H(H^{\cdot}) - H(RX-H) \quad (1)$$

$$IP = H\left((RX-H)^{+\cdot}\right) + H(e^-) - H(RX-H) \quad (2)$$

$$PDE = H(RX^{\cdot}) + H(H^+) - H\left((RX-H)^{+\cdot}\right) \quad (3)$$

$$PA = H(RX^-) + H(H^+) - H(RX-H) \quad (4)$$

$$ETE = H(RX^{\cdot}) + H(e^-) - H(RX^-) \quad (5)$$

Calculation of vibrational frequencies, using the unrestricted open shell level UB3LYP/6-311G(d,p), was conducted for the generated radicals RX° and $RX\text{-}H^{+\circ}$. It should be noted that

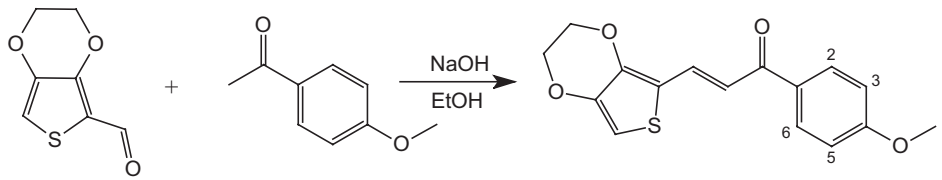

Scheme 2: Synthesis scheme of the studied chalcone.

no significant change was observed in results obtained after geometry optimization for the said radicals.

Anti-tyrosinase activity

Tyrosinase inhibitory activity of *Mushroom* species was investigated spectrophotometrically as given by Masuda *et al.*[26] with minor changes. l-DOPA was used as substrate, whereas kojic acid was used as standard. Thus, 150 µL of 100 mM sodium phosphate buffer (pH 6.8), 10 µL of sample solution dissolved in methanol at different concentrations, and 20 µL tyrosinase enzyme solution in buffer were mixed and incubated for 10 min at 37°C, and then 20 µL of l-DOPA was added. The mixture was incubated a second time for 10 min at 37°C before reading its absorbance at 475 nm in a 96-well microplate.

$$\text{Tyrosinase inhibition } (\%) = \frac{A_{Control} - A_{Sample}}{A_{Control}} \times 100$$

Molecular docking

Arguslab 4.0.1 software[27] was used to estimate the affinity between tyrosinase and the tested molecules and to analyze the intermolecular interactions that are involved. Thus, a molecular docking calculation was carried out considering the flexibility of ligands. The stability of the enzyme–ligand complex is inversely related to its Gibbs free energy ($\Delta G_{binding}$) calculated by the Ascore function, which is implemented in Arguslab and is given by:

$$\Delta G_{binding} = \Delta G_{vdW} + \Delta G_{hydrophobic} + \Delta G_{H\text{-}bond} + \Delta G_{H\text{-}bond(chg)} + \Delta G_{deformation} + \Delta G^{\circ}$$

where, ΔG_{VdW} represents the van der Waals interaction between the protein and the ligand, $\Delta G_{hydrophobic}$ represents the hydrophobic effect, $\Delta G_{H\text{-}bond}$ and $\Delta G_{H\text{-}bond(chg)}$ are assigned to the hydrogen bonding and the hydrogen bonding involving charged donor and/or acceptor groups between the ligand and the protein, respectively, the deformation effect is given by $\Delta G_{deformation}$, and finally $\Delta G°$, which corresponds to the effects of the translational and rotational entropy loss during complexation.

Already modeled and optimized at the B3LYP/6-311G(d,p) level of the DFT theory, the ligands will be directly used. As for the three-dimensional structure of the enzyme, it is obtained from the Research Collaboratory for Structural Bioinformatics protein data bank (http://www.rcsb.org/). Therefore, the entry 1wx2, which meets the selection criteria of a protein data bank file, was proposed by Warren *et al.*[28] and which was used in many similar studies,[29,30] was selected. Water molecules and the caddie protein were removed. Hydrogen atoms were added and docking parameters were adapted as the binding site bounding box dimensions, which were equal to: 20 × 20 × 15 Å^3. The docking engine ArgusDock was chosen and the default value of grid resolution (0.4 Å) was kept. The intermolecular interactions analysis was perfected using the discovery studio 4.0 software.[31]

Lipinski's rule of five

Given by Lipinski *et al.*[32] in 1997, the rule of five is based on certain criteria to estimate druglikeness of a molecule having a pharmacological activity. These criteria are log *P* lower than 5, number of hydrogen bond donors less than 5, number of acceptors of hydrogen bonds less than 10, and molecular weight not exceeding 500 Da. The rule is used in drug design to preselect molecules presenting good absorption, distribution, metabolism, and excretion (ADME) properties that must have a medicament in the organism. We have used Molinspiration property calculator (http://www.molinspiration.com) to calculate the four parameters of Lipinski's rule in addition to the number of rotatable bonds that have to be inferior to 10 to have a good oral bioavailability.[33]

Results and Discussion

Antioxidant activity assessment

Results of the three used methods are present in Table 1.

1,1-Diphenyl-2-picrylhydrazyl scavenging activity method

Among the tested compounds, OX2 and OX1 showed the highest activity, with a percentage of inhibition of 74.63 ± 2.94 and 34.50 ± 1.56, respectively. The first value is quite close to those of BHA and BHT.

Cupric reducing antioxidant capacity method

The obtained results from the CUPRAC assay showed that OX1 and OX2 presented a better antioxidant activity than the tested standards, with an $A_{0.50}$ of 2.60 ± 0.16 µg/mL and 3.62 ± 0.31 µg/mL, respectively. In a global way, the CUPRAC antioxidant power order obtained for the studied oximes was: OX1 > OX2 > OX4 > OX3 > OX5.

Ferric reducing antioxidant power method

FRAP results showed that OX2, once again have the best reducing power activity among the tested molecules with an $A_{0.5}$ of 6.89 ± 0.23 µg/mL, a comparable value to those of the used standards. If OX5 presented a relatively weak FRAP activity, no significant activity was observed for OX4, OX1, and OX3.

Molecular descriptors calculation

1. Comparison with DPPH scavenging assay results: For all molecules in vacuum, the following sequence: BDE > IP > PA, is respected, which favors a HAT mechanism, whereas the SPLET mechanism is preferred for the five molecules in ethanol, as the three descriptors are ordered in the flowing manner: PA > BDE > IP [Table 2]. This is in concordance with literature where HAT mechanism is favored in nonpolar media and SET-PT or SPLET mechanisms are preferred in polar ones because of the charged species creation.[34] Notice that three of our molecules (OX1, OX2, and OX4) present each two transferable hydrogen atoms. In the case of OX4 and OX2, these atoms will be noted H_a and H_b, as shown in

Figure 1. To determine which atom transfer is favorable in each case, we have to compare the corresponding PA values. Remember that PA was found to be the determinant descriptor in ethanol phase. Thus, for OX1, the results showed that the N-H bond proton departure is more favorable compared to that of the O-H bond one. This may be due to the fact that the departure of the proton from the N-H bond creates a stabilizing resonance at the two indole rings. Concerning the two other oximes, the PA value of the H_b proton is inferior to the H_a one for OX4, whereas the opposite situation is observed for OX2. This indicates that the most labile proton is H_b for OX4 and H_a for OX2. Overall, PA values' order is: OX2-H_a < OX4-H_b < OX1-N < OX3 < OX5. This is in perfect concordance with the experience [Table 1]. On the contrary, calculations conducted in gas phase showed the following sequence of BDE values (determinant descriptor in the gas phase): OX1-N < OX3 < OX5 < OX2-H_a < OX4-H_a.

2. Comparison with CUPRAC assay results: As aforementioned for this electron transfer based test, the antioxidant activity is inversely proportional to the IP values of molecules. In ethanol, IP of our oximes are ordered as: OX1 < OX2 < OX3 < OX4 < OX5. This constitutes a nearly perfect accord between the theoretical approach and the experimental one.

Table 1: Antioxidant assays (1,1-diphenyl-2-picrylhydrazyl scavenging activity, ferric reducing antioxidant power test, and cupric reducing antioxidant capacity test) results. The corresponding antioxidant standard values are reported

Compound	Antioxidant activity		
	DPPH assay % of inhibition	CUPRAC assay A0.50 (µg/mL)	FRAP assay A0.50 (µg/mL)
OX1	34.50 ± 1.56	2.60 ± 0.16	>200
OX2	74.63 ± 2.94	3.62 ± 0.31	6.89 ± 0.23
OX4	4.56 ± 0.45	9.52 ± 5.62	>200
OX3	6.98 ± 4.36	13.71 ± 3.07	>200
OX5	NA[a]	>200	187.25 ± 9.89
BHA	84.18 ± 0.10	5.35 ± 0.71	6.77 ± 1.15
BHT	94.00 ± 0.31	8.97 ± 3.94	5.39 ± 0.91

[a]NA = no absorbance

$A_{0.50}$ (µg/mL), sample concentration indicating 0.5 absorbance

The percentage of inhibition was calculated at 100 µg/mL of the sample concentration

Anti-tyrosinase activity

Three of the tested oximes showed an anti-tyrosinase activity. OX4 revealed the highest activity among these compounds with 51.89% ± 6.04% of the enzyme amount inhibited at 200 µg/mL of sample's concentration. At the same concentration, OX3 and OX1 showed less activity with an inhibition percentage of 32.95 ± 11.07 and 10.33 ± 7.17, respectively [Table 3]. No inhibition effect was observed in the case of OX2 and OX5.

Molecular docking

From the molecular docking calculation results [Table 3], all the tested molecules show an importance with respect to the used standard (kojic acid). This means that they may constitute a thermodynamically favorable complex.

As well, the enzyme–ligand interaction analysis showed that the three molecules presenting an inhibitory effect were docked in enzyme's active site pocket [Figure 2], which is located around the dicopper center (Cu^A and Cu^B).[35] OX4 presented a hydrogen bond with Glu182 and three hydrophobic interactions, two of them with Trp184 and a third with Ile42, whereas OX3 formed a hydrophobic interaction with Trp184. Then, the binding mode of OX1 consisted of a three hydrogen bonds with Asn191, Ser206, and Thr203, respectively, and two hydrophobic interactions with His194 and His54 [Table 4].

Table 3: Percentage of inhibition (at 200 µg/mL of sample) and ΔGbinding values of the tested oximes

Molecule	% of inhibition at 200 µg/mL[a]	ΔGbinding (kcal/mol)
OX4	51.89 ± 6.04	−6.766
OX3	32.95 ± 11.07	−6.204
OX1	10.33 ± 7.17	−6.631
OX2	NA[b]	ND[c]
OX5	NA	ND
Kojic acid	66.95 ± 2.24	−6.031

[a]Values expressed are mean ± standard deviation (SD) of three parallel measurement ($P < 0.05$)

[b]NA = no absorbance

[c]NAP = not done

Table 2: Molecular descriptors (bond dissociation enthalpy, ionization potential, and protein affinity) values (kJ/mol) calculated in vacuum and in solvent (ethanol), for the tested molecules and standards

Molecule	BDE		IP		PA	
	Vacuum	Solvent	Vacuum	Solvent	Vacuum	Solvent
OX4-H_b	414.94	376.58	796.26	532.46	1525.02	239.60
OX2-H_b	411.29	404.65	773.22	493.43	1472.35	266.37
OX4-H_a	389.84	367.04	796.26	532.46	1470.62	269.44
OX2-H_a	369.87	378.50	773.22	493.43	1450.15	229.28
OX5	369.57	355.92	655.43	1067.55	1483.88	271.95
OX1	356.86	390.40	758.21	473.23	1535.97	294.49
OX3	351.29	375.16	835.91	500.15	1500.64	258.02
OX1-N	351.26	402.80	758.21	473.23	1438.15	254.45

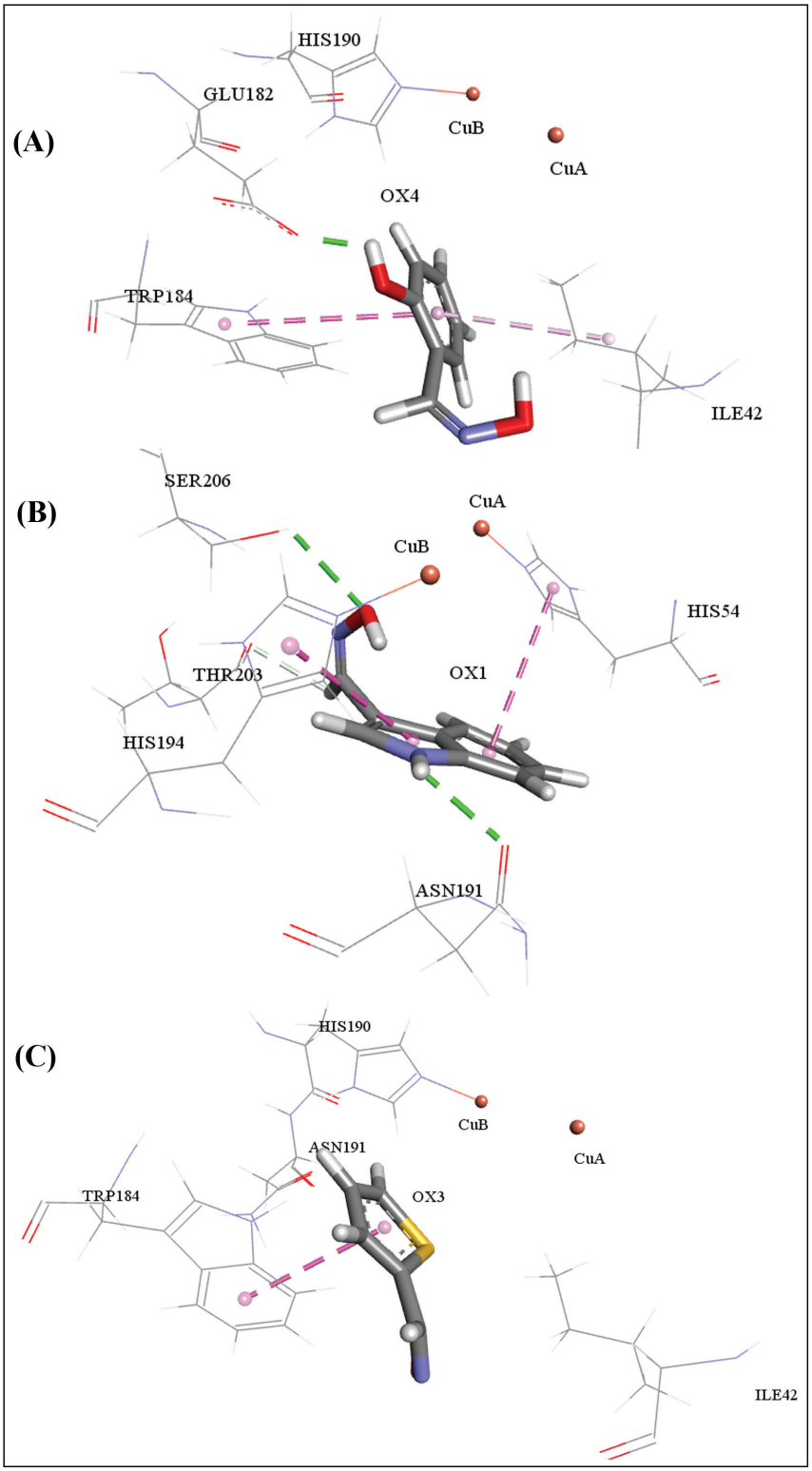

Figure 2: Tyrosinase interactions with OX4 (A), OX3 (B), and OX1 (C). Ligands are represented as ball and stick, whereas all other residues are displayed as lines except those interacting with the ligand. The ochre balls correspond to the copper ions

Lipinski's rule of five

All our molecules fulfil the Lipinski's rule criteria and the extra condition on the number of rotatable bonds [Table 5], suggesting their good pharmacokinetic permeability and their oral bioavailability, which may allow them to constitute lead compounds for oxidative stress diseases therapies.

Table 4: Favorable intermolecular interactions between the three active oximes (OX4, OX3, and OX1) and the enzyme (tyrosinase)

Molecule	Hydrogen bonding		Hydrophobic interactions	
	Interaction	Distance (Å)	Interacting residue	Distance (Å)
OX4	OH···O:Glu182	1.870	Trp184	5.115
			Trp184	5.879
			Ile42	4.540
OX3	/	/	Trp184	4.161
OX1	NH···O:Asn191	2.387	His194	4.395
	NO···HO:Ser206	2.667	His54	5.013
	CH···O:Thr203	2.656		

Table 5: Evaluation of the druglikeness properties of the five molecules by Molinspiration Property Calculator

Molecule	Log P[a]	MW[b]	nON[c]	nOHNH[d]	Nrotb[e]
OX1	2.51	160.18	3	2	1
OX2	3.46	187.20	3	2	1
OX3	2.25	127.17	2	1	1
OX4	2.30	137.14	3	2	1
OX5	3.48	317.37	5	1	4

[a]Log P = octanol–water partition coefficient
[b]MW = molecular weight
[c]nON = number of acceptor hydrogen bonds
[d]nOHNH = number of donor hydrogen bonds
[e]Nrotb = number of rotatable bonds

Conclusion

The obtained results from the used experimental tests illustrate that the majority of our oximes showed a good antioxidant activity, even better than the customary used antioxidant standards, for OX2 and OX1. The most thermodynamically favorable DPPH scavenging mechanism was investigated theoretically and the SPLET mechanism was designated for the tested compounds, in ethanol phase, and HAT mechanism for the gas phase. The obtained values of PA, which is the determinant descriptor for SPLET mechanism, are ordered in perfect agreement with the experience. On the contrary, for CUPRAC test, results were in harmony with the calculated IP. Moreover, OX3, OX4, and OX1 revealed an anti-tyrosinase activity. Nevertheless, no inhibition effect against this enzyme was observed for OX2 and OX5. This same result is obtained theoretically through a molecular docking calculation. The submission of our molecules to Molinspiration software showed that they fulfill the Lipinski's rule of five. From all these results, we can say that our compounds could be used as antioxidant agents even in pharmacological, cosmetic, or food industries. Nevertheless, further clinical tests are needed to fully validate this conclusion.

Financial support and sponsorship

This study was supported by the Directorate General of Scientific Research and Technological Development of the Algerian Ministry of Higher Education and Scientific Research (DGRSDT-MESRS, Algeria).

Conflicts of interest

There are no conflicts of interest.

References

1. Potaniec B, Grabarczyk M, Stompor M, Szumny A, Zieliński P, Żołnierczyk AK, *et al*. Antioxidant activity and spectroscopic data of isoxanthohomol oxime and related compounds. Spectrochim Acta Part A Mol Biomol Spectrosc 2014;118:716-23.
2. Tallam SK, Latha DS, Sowjanya G, Swathi P, Bharathi V, Sreenivasulu V. Synthesis, characterization and pharmacological evaluation of substituted N-benzyl isatin 3-oximes. J Global Trends Pharm Sci 2016;7:3057-64.
3. Puntel GO, Gubert P, Peres GL, Bresolin L, Rocha JBT, Pereira ME, *et al*. Antioxidant properties of oxime 3-(phenylhydrazono) butan-2-one. Arch Toxicol 2008;82:755-62.
4. Türkkan B, Ozyürek M, Bener M, Güçlü K, Apak R. Synthesis, characterization and antioxidant capacity of naringenin-oxime. Spectrochim Acta A Mol Biomol Spectrosc 2012;85:235-40.
5. Kassa J. Review of oximes in the antidotal treatment of poisoning by organophosphorus nerve agents. J Toxicol Clin Toxicol 2002;40:803-16.
6. Leopoldini M, Russo N, Toscano M. The molecular basis of working mechanism of natural polyphenolic antioxidants. Food Chem 2011;125:288-306.
7. Musialik M, Litwinienko G. Scavenging of DPPH* radicals by vitamin E is accelerated by its partial ionization: The role of sequential proton loss electron transfer. Org Lett 2005;7:4951-4.
8. Fifen JJ, Nsangou M, Dhaouadi Z, Motapon O, Jaidane N. Solvent effects on the antioxidant activity of 3,4-dihydroxyphenylpyruvic acid: DFT and TD-DFT studies. Comput Theor Chem 2011;966:232-43.
9. Apak R, Güçlü K, Demirata B, Özyürek M, Çelik SE, Bektaşoğlu B, *et al*. Comparative evaluation of various total antioxidant capacity assays applied to phenolic compounds with the CUPRAC assay. Molecules 2007;12:1496-547.
10. van Gelder CW, Flurkey WH, Wichers HJ. Sequence and structural features of plant and fungal tyrosinases. Phytochemistry 1997;45:1309-23.
11. Khan V. Effect of kojic acid on the oxidation of DL-DOPA, norepinephrine, and dopamine by mushroom tyrosinase. Pigment Cell Res 1995;8:234-40.
12. Rho HS, Baek HS, Ahn SM, Kim MK, Ghimeray AK, Cho DH, *et al*. Synthesis and biological evaluation of kojyl thioether derivatives as tyrosinase inhibitors. Bull Korean Chem Soc 2010;31:2375-8.
13. Ley JP, Bertram HJ. Hydroxy- or methoxy-substituted benzaldoximes and benzaldehyde-O-alkyloximes as tyrosinase inhibitors. Bioorg Med Chem 2001;9:1879-85.
14. Radhakrishnan S, Shimmon R, Conn C, Baker A. Integrated kinetic studies and computational analysis on naphthyl chalcones as mushroom tyrosinase inhibitors. Bioorg Med Chem Lett 2015;25:4085-91.
15. Frisch MJ, Trucks GW, Schlegel HB, Scuseria GE, Robb MA, Cheeseman JR, *et al*. Gaussian 09, Revision E.02. Wallingford CT: Gaussian; 2016.
16. Dennington R, Keith TA, Millam JM. GaussView, Version 5.0.9. Shawnee Mission, KS: Semichem; 2016.
17. Greene TW, Wuts PGM. Protective Groups in Organic Synthesis. 4th ed. New York: John Wiley & Sons; 2006.
18. Blois MS. Antioxidant determinations by the use of a stable free radical. Nature 1958;81:1199-200.

19. Apak R, Güçlü K, Ozyürek M, Karademir SE. Novel total antioxidant capacity index for dietary polyphenols and vitamins C and E, using their cupric ion reducing capability in the presence of neocuproine: CUPRAC method. J Agric Food Chem 2004;52:7970-81.
20. Oyaizu M. Studies on products of browning reactions: Antioxidative activities of browning reaction prepared from glucosamine. Jpn J Nutr 1986;44:307-15.
21. Cancès E, Mennucci B, Tomasi J. A new integral equation formalism for the polarizable continuum model: Theoretical background and applications to isotropic and anisotropic dielectrics. J Chem Phys 1997;107:3032-41.
22. Jabbari M, Mir H, Kanaani A, Ajloo D. Kinetic solvent effects on the reaction between flavonoid naringenin and 2,2-diphenyl-1-picrylhydrazyl radical in different aqueous solutions of ethanol: An experimental and theoretical study. J Mol Liq 2014;196:381-91.
23. Bartmess JE. Thermodynamics of the electron and the proton. J Phys Chem 1994;98:6420-4.
24. Bamonti L, Hosoya T, Pirker KF, Böhmdorfer S, Mazzini F, Galli F, *et al*. Tocopheramines and tocotrienamines as antioxidants: ESR spectroscopy, rapid kinetics and DFT calculations. Bioorg Med Chem 2013;21:5039-46.
25. Tošović J, Marković S, Milenković D, Marković Z. Solvation enthalpies and Gibbs energies of the proton and electron: Influence of solvation models. J Serb Soc Comput Mech 2016;10:66-76.
26. Masuda T, Yamashita D, Takeda Y, Yonemori S. Screening for tyrosinase inhibitors among extracts of seashore plants and identification of potent inhibitors from *Garcinia subelliptica*. Biosci Biotechnol Biochem 2005;69:197-201.
27. Thompson MA. Molecular docking using ArgusLab, an efficient shape-based search algorithm and the AScore scoring function. ACS Meeting, Philadelphia, PA, 2004.
28. Warren GL, Do TD, Kelley BP, Nicholls A, Warren SD. Essential considerations for using protein-ligand structures in drug discovery. Drug Discov Today 2012;17:1270-81.
29. Lam KW, Syahida A, Ul-Haq Z, Abdul Rahman MB, Lajis NH. Synthesis and biological activity of oxadiazole and triazolothiadiazole derivatives as tyrosinase inhibitors. Bioorg Med Chem Lett 2010;20:3755-9.
30. Nithitanakool S, Pithayanukul P, Bavovada R, Saparpakorn P. Molecular docking studies and anti-tyrosinase activity of Thai mango seed kernel extract. Molecules 2009;14:257-65.
31. Dassault Systems Biovia, Discovery Studio Modeling Environment, Release 2017. San Diego, CA: Dassault systèmes; 2016.
32. Lipinski CA, Lombardo F, Dominy BW, Feeney PJ. Experimental and computational approaches to estimate solubility and permeability in drug discovery and development settings. Adv Drug Deliv Rev 1997;23:3-25.
33. Veber DF, Johnson SR, Cheng HY, Smith BR, Ward KW, Kopple KD. Molecular properties that influence the oral bioavailability of drug candidates. J Med Chem 2002;45:2615-23.
34. Zhang H-Y, Ji H-F. How vitamin E scavenges DPPH radicals in polar protic media. New J Chem 2006;30:503-4.
35. Matoba Y, Kumagai T, Yamamoto A, Yoshitsu H, Sugiyama M. Crystallographic evidence that the dinuclear copper center of tyrosinase is flexible during catalysis. J Biol Chem 2006;281: 8981-90.